Flake Powder Metallurgy

Flake powder metallurgy (FPM) including different processing routes, conventional FPM (C-FPM), slurry blending (SB), shift-speed ball milling (SSBM), and high-shear pre-dispersion and SSBM (HSPD/SSBM). The name of FPM was derived from the use of flake metal powders obtained by low-speed ball milling (LSBM) from spherical powder. The uniformity of reinforcement distribution leads to increased strength and ductility. Powder is the basic unit in PM, especially advanced PM, and its control is key to various new PM technologies. The FPM is a typical method for finely controlling the powder shape through low-energy ball milling (LEBM) to realize the preparation of advanced material structures.

1. Introduction

With the rapid development of metal matrix composites (MMCs) and especially aluminum matrix composites (AMCs), traditional casting, infiltration, plastic forming, and other methods showed a limited ability to meet the requirements of preparation and processing of new aluminum matrix composites. New powder metallurgy technology, large plastic deformation, and material addition manufacturing have a high controllability and unique role in the preparation and processing of AMCs, which has been widely noted by advanced researchers.

In recent decades, many efforts such as powder metallurgy (PM) [1][2][3], severe plastic deformation (SPD) [4][5][6][7][8], nanoscale dispersion (NSD) [9][10], in situ chemical vapor deposition (CVD) [11][12], and ball milling followed by post-sintering processes such as forging, extrusion, or rolling [13][14][15][16][17][18][19] have been undertaken to fabricate MMCs, especially AMCs. Among all the proposed techniques, the PM route has been identified as very promising in order to obtain optimal second phase distributions [20][21][22]. The basics of this route comprise the deformation, cold-welding and balanced stages [23]. At the deformation stage, ductile Al powders flatten as a consequence of intense collisions of steel balls with powder particles, consequently providing a larger specific surface compared to spherical particles. Reinforcement clusters are fractured and then dispersed onto the surface of the flattened powder [24][25][26]. During the cold-welding stage, flattened powders are cold-welded into coarser reinforcement-metal powder particles decorated by reinforcement at the welded seams. It should be noted that once reinforcements are inserted, their further dispersion becomes more and more difficult. Therefore, the minimum necessary time for cold-welding should be precisely set [27][28].

Powder metallurgy (PM) technology can control the interface of the composite at temperatures well below the melting point of the aluminum matrix, thereby allowing for avoidance of the natural agglomeration of micro-reinforcements into the melt and the floating or settling of reinforcements due to differences between the density values of the melt and the second phase. At the same time, the AMCs have a smaller matrix structure than the liquid phase method. As the basic unit of PM technology, control of powder is key to various new PM technologies.

Some technologies use the reaction activity resulting from the high specific surface area of powder and the external input energy. The dispersion of nano-reinforcements is accomplished through an in situ reaction, such as the reaction of spray deposition of atomized droplets and reactant [29] or the mechano-chemical reaction of powder and reactant through high-energy ball milling [30]. Some PM technologies can disperse the reinforcement, control the shape of the powder and refine the powder grains through high deformation during ball milling, such as mechanical alloying of the reinforcement by long-term high-energy ball milling (HEBM) and low-temperature ball milling such as cryo-milling [31][32][33]. The HEBM route has demonstrated its effectiveness in the destruction of the oxides layers, providing optimal interface bonding between the second reinforcing phase and the matrixes. However, the severe deformation due to ball milling can lead to remarkable damage in very brittle reinforcements such as CNTs.

In general, most of the new PM technologies have been developed to realize the new component design or structural design of AMCs. For example, flake PM (FPM) is a typical method for fine control of powder shape LEBM of mostly ≤ 200 rpm [24][27][34][35][36], and then for the preparation of the composite structure. The method not only is characterized by a

very high specific surface area and flat surface, but also provides sufficient space for the surface in situ reaction [37][38] and surface dispersion [26][39][40] to the reinforcement, and can induce flake nano-grain (NG) or ultrafine grain (UFG) in the powder. This fine microstructure can then be retained in the bulk material. Depending on whether or not the flake shape is destroyed during the powder consolidation process, a nano-reinforced body dispersion structure [25][40][41][42][43] or a layered configuration [44][45][46][47] can be formed, respectively.

The obtaining of sound mechanical properties in nano-reinforced AMCs can be achieved only if second-phase optimal dispersion is realized during processing [3][24][48][49]. The second requirement effectively maintains the structural integrity of the nano-dispersions, especially for CNT and graphene [27][50][51]. The third requirement is interfacial bonding between the nano-dispersal surfaces and the matrix material [19][25][52]. It is interesting to note that the alignment of the nano-dispersoids has a remarkable influence on the mechanical properties of metal matrix composites [53]. The new PM technologies, namely FPM, as a powder-smart severe plastic deformation (SPD) method will enable us to overcome the obstinate roadblocks in UFG alloys and MMCs caused by poor dislocation storage and weak strain hardening ability. FPM, as a bottom-up approach, could fulfill a flaky powder geometry known as the building blocks of bulk advanced materials, which was hitherto believed impossible.

The PM route for MMCs production comprises the following main steps: powder processing and consequent powder consolidation. Metal powders are blended with reinforcements by means of techniques such as conventional FPM (C-FPM) [35][47][54], slurry blending (SB), vapor-based synthesis, shift-speed ball milling (SSBM), and high-shear pre-dispersion and SSBM (HSPD/SSBM), which are then followed by various consolidation routes of the mixture such as hot extrusion [27][55], spark plasma sintering [47][56][57], friction stir processing [58][59], hot rolling [19][46][60], and others [5][36]. Significant advances can be underlined in the field of solid-phase powder metallurgy (PM) techniques [47]. The PM based methods include HEBM [19][46][55], FPM [24][34], liquid phase ball milling [24][61], nanoscale dispersion methods [9][10], molecular level mixing [62][63] and in-situ CNTs production combined with low-energy ball milling [11][37][64], and others [65]. These methods sometimes require large time consumption when used on an industrial scale. Therefore, it is fundamental to review recent advances in powder-based processing techniques such as FPM. This review specifically focuses on the different FPM approaches, namely C-FPM, SB, SSBM, and HSPD-SSBM. After reviewing the recent advances in FPM approaches, the potential for further optimization and development is indicated.

The main developed powder metallurgy routes are based on the employment of starting spherical powders in order to allow dense compaction of the formed blocks. By contrast, FPM is based on the employment of flake-shaped reinforcements that can be aligned by formation through hot compaction and rolling or extrusion. During flake powder metallurgy, the main processing steps are the precise preparation of flake reinforcements, their proper mixing, consolidation, and alignment.

From the crystal plasticity perspective, the BM process is known as a micro-plastic deformation process, affected by rotational speed and rotational time [2][27][66][67]. Generally, the collision forces between the milling balls and reinforcement and matrix powders with all their complexity, including compressing and shearing forces, are the origin of the BM process evolution [27][68]. Specifically, compression leads to the powder's deformation, flattening and fragmentation, as well as final cold welding. In contrast, shearing effectively promotes the breaking of contamination skins such as alumina skin in Al powders and reinforcement clusters, resulting in uniform dispersion of reinforcements.

2. Conventional Flake Powder Metallurgy (C-FPM)

The FPM via typical dry milling is introduced as powder BM in a dry jar. Specifically, the ingredients blended in the jar are reinforcement, matrix powder, steel balls, and usually a processing agent such as stearic acid, ethanol or similar. The process of flaking for spherical metal powders under the C-FPM route is performed through micro-rolling (ball milling) the starting powders (Figure 1a).
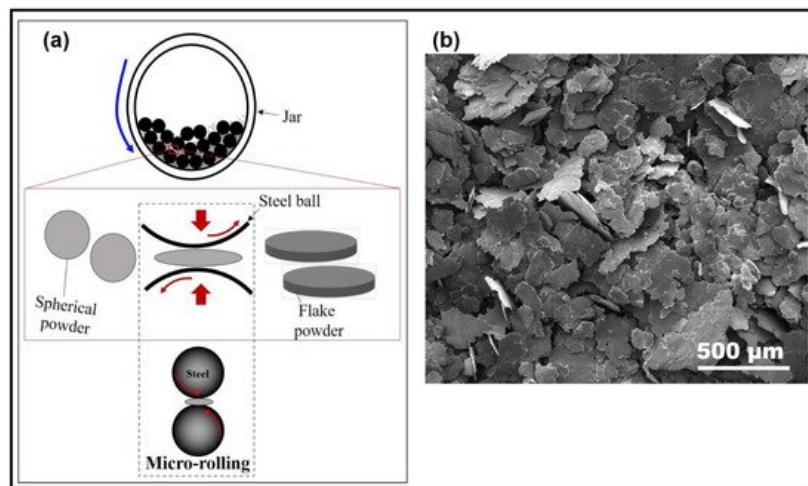
Figure 1. (**a**) Schematic of micro-rolling process, (**b**) SEM images of CNT/Al flakes under C-FPM route.

In current practice, for the first time, the LSBM process is considered a kind of rolling process, but on a micro scale—namely, micro-rolling—because: (1) the LSBM process causes plastic deformation of initial powders, thus leading to significant effects on the geometry of the powders; specifically, particles flatten via a process which is similar to the one which is performed in the conventional rolling process, (2) milling balls can be considered similar to conventional rollers but with a much smaller size, and (3) despite the difference in the source of the generation of imposed stresses, deformation occurred originating from shear stresses upon the powders.

2. Flake Powder Metallurgy via Slurry Blending (FPM-SB)

The strategy of using a slurry-based dispersion process of the reinforcement has emerged as a mighty new route in overcoming the prerequisites needed to produce advanced AMMs [39][69]. In this technique, the particles' morphology is modified from three-dimensional spheres to two-dimensional flakes. Subsequently, the surface is modified through organic solutions such as polyvinyl alcohol (PVA) or ethanol. In this way, the flakes can easily attract the second phases onto their surfaces. The produced composite is then compacted and sintered, as illustrated in Figure 2a.
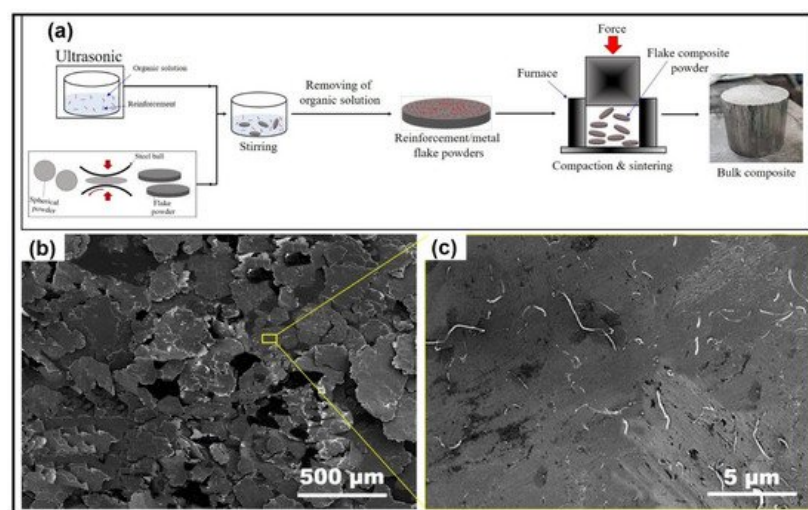

Figure 2. (**a**) Schematic of slurry-based dispersion process, (**b**,**c**) SEM images of CNT/Al flakes under FPM-SB route.

As a matter of fact, the FPM-SB CNT/Al nanocomposite showed tensile stress of 375 MPa with strain to fracture around 12%, very high when compared to corresponding material produced via conventional PM (330 MPa strength and 6% ductility, Figure 3a) [24][26]. The high-level ordering nanolaminates of flake-shaped building blocks was reported as the key factor in significantly increased tensile strength and ductility when compared with nanocomposites with the same matrix and with non-uniform distribution of CNTs. Moreover, Figure 3b depicts that the advantage of FPM over other methods such as nanoscale dispersion (NSD) [9], low-energy blending (LEB), and others can be obtained through the comparison of the strengthening effects of CNTs®. In fact, an incredible strengthening of the efficiency of CNTs is obtained through FPM thanks to the homogeneous and individual distribution of CNTs in the Al matrix, originating from the high compatibility of Al powders with CNTs [24][70].
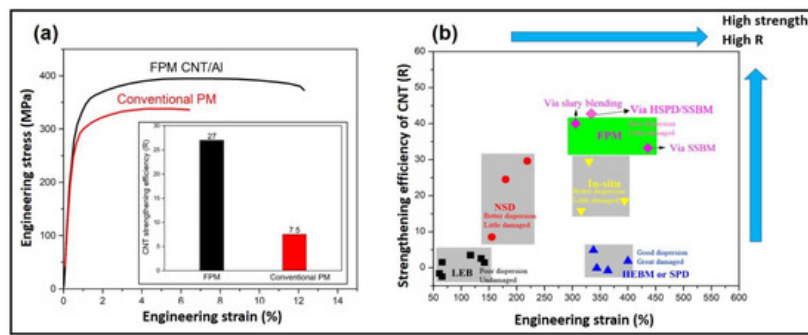
Figure 3. Tensile properties of CNT/Al nanocomposites (**a**) loading with 1 vol.% CNTs and fabricated by conventional PM and flake PM (inset shows the relevant strengthening efficiencies of CNTs), (**b**) The strengthening efficiency and tensile strength for CNT/Al composites fabricated by various methods, the data were drawn based on recent reviews [22][24][48][71] [72].

Despite the numerous advantages of FPM via slurry blending, through the application of the abovementioned method to fabricate AMCs with high nano-reinforcement percentages of CNT [3], SiO_2 [73], etc., the ductility of the composite also decreased dramatically. Thanks to high nano-reinforcement percentages, various layers of nano-reinforcement can be bonded and overlapped through slurry-based dispersion, even if this leads to difficult bonding between neighboring Al nanoflakes. Hence, the main goal of the FPM processing route for the production of MMCs is the combination of reinforcement dispersion with the structural properties and matrix-second phases bonding.

3. Flake Powder Metallurgy via Shift Speed-Ball Milling (FPM-SSBM)

The correlation between the CNTs distribution, consequent bonding and final mechanical strength of the composites has been the subject of in-depth study by many scientists [35][65][67][74][75][76][77][78]. Here, the different BM conditions (low- and high-energy) affecting the final properties of AMCs are illustrated in order to optimize the different milling strategies. To this end, recently, Xu et al. [27] proposed a new flake powder metallurgy route via a SSBM strategy. In this strategy, LSBM was applied for very long times in order to obtain aluminum flat flakes with very uniform distribution of reinforcements without damage. The results are compared with those of HSBM in order to produce cold-welded lamellar particles with acceptable CNT/Al bonding and inter-flake bonding, as shown in Figure 4a. Specifically, LSBM allowed for mild ball-to-powder contact and very slow flattening of spherical metal powders into flake-shaped powders. This provided enough time for nano-reinforcements to be optimally dispersed on the surface of metal flakes with low damage to structure integrity of nano-reinforcements, especially carbon-based ones such as CNT or graphene; HSBM showed much more pronounced collisions and cold welding of Al flakes into cake-like particles with a clear laminated structure, as seen in Figure 4b,c, leading to clustered nano-reinforcements within the welded metal particles. In this case, very pronounced damage to reinforcements resulted.
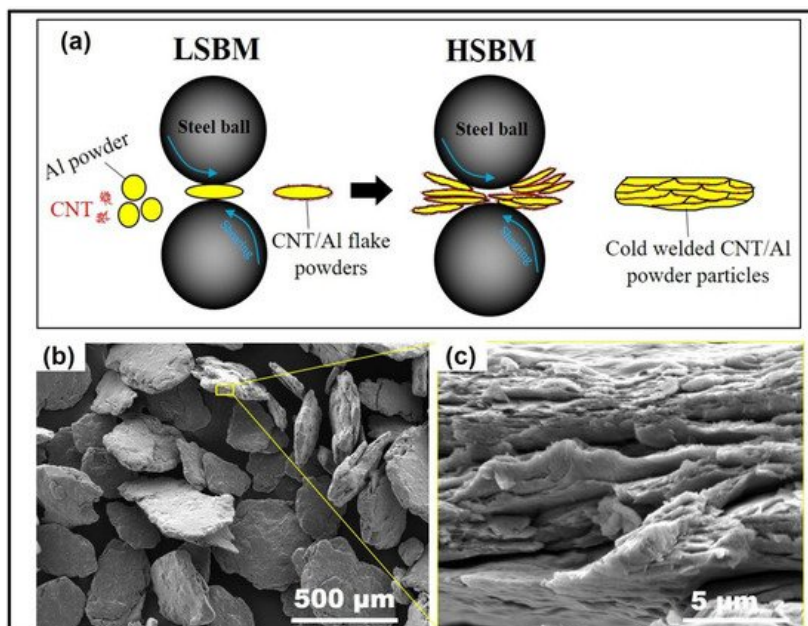

Figure 4. (**a**) Illustration of co-deformation/dispersion mechanisms of CNT/Al powders during FPM-SSBM, (**b**,**c**) SEM images of CNT/Al particles obtained via FPM-SSBM route.

Further developments demonstrate that SSBM, where different powder deformation mechanisms are obtained as a consequence of various milling speeds, produces a high strength of up to 1.5% of CNTs. The strength and ductility levels are much higher compared to sole LSBM or HSBM [27]. As a matter of fact, the optimal combination of reinforcement distribution, structural integrity and matrix-second-phase bonding can be obtained through a new SSBM process known as FPM-SSBM.

Most composites exhibited a strength–ductility dilemma and these data are all placed under a typical "banana shaped" curve (Figure 5). However, the strength–ductility results of the SSBM route for CNT/Al composite overcome the blue belt in the graph, demonstrating improved mechanical properties. Therefore, FPM-SSBM is a very effective route for this materials' processing. Comparing previous studies with FPM-SSBM revealed that, with conventional milling processes, it was difficult to fabricate CNT/Al composite with uniform CNT dispersion and good bonding without reducing CNT integrity [70]. In contrast, SSBM enhanced the mechanical property of CNT/Al composites by combining the advantages of LSBM, which included mild ball-to-powder collision and slow flattening of spherical Al powders into flakes, with those of HSBM, which included a much stronger collision and cold welding of Al flakes, and avoiding the adverse factors introduced by LSBM and HSBM, which were unhealed insufficient bonding between Al flakes, and many local brittle areas with CNT clusters or forming brittle Al_4C_3, respectively. Hence, FPM is known as a smart technology of SPD materials based on a bottom-up approach.
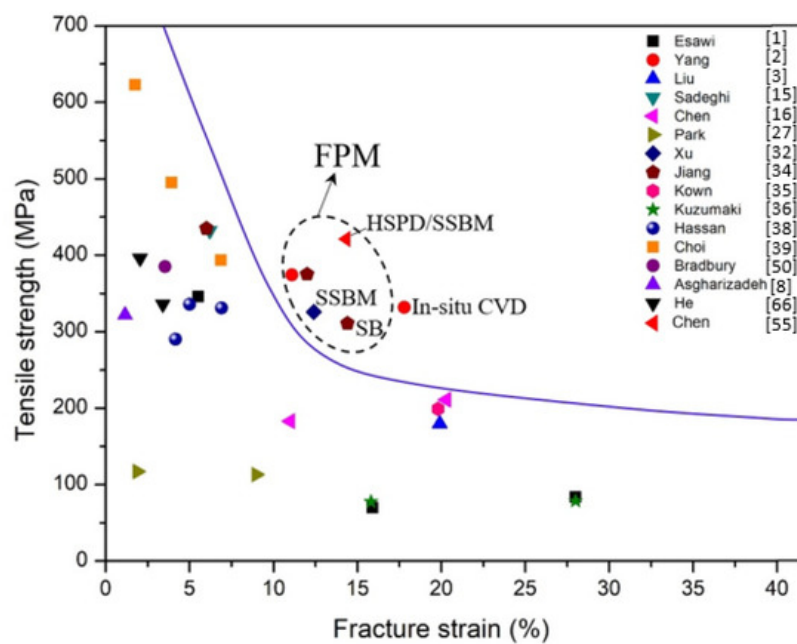

Figure 5. Representative tensile properties of FPM-SSBM CNT/Al composites [27].

4. Flake Powder Metallurgy High-Shear Pre-Dispersion and SSBM (FPM-HSPD/SSBM)

De-agglomeration of CNTs before ball milling results in an optimal solution to gain good reinforcements dispersion. However, this good dispersion is difficult to obtain via the traditional SB route because of the easier re-aggregation of second phases during drying. Presently, many AMCs' processing routes show some limitations in the reinforcement dispersion, especially in the case of high reinforcement percentages. In addition, as the reinforcement percentage increases, the control of interfacial reactions becomes more difficult [65]. The PM-based methods include high-energy ball milling [19][46][54], flake powder metallurgy [24][34], liquid-phase ball milling [24][61], nanoscale dispersion method [9][10], molecular level mixing [62][63] and the in-situ formation of CNTs in combination with low-energy ball milling [11][37][64], etc. [65]. Nevertheless, these solutions require energy and time consumption which is incompatible with industrial production. Therefore, pre-dispersion optimized methods are fundamental in this direction [34][52][79][80].

5. Promising BM Techniques

In addition to the production methods of flake powder mentioned above, two other techniques based on controlling ball movement—namely, electrical discharge-assisted mechanical milling (EDAMM) and magnetic mechanical milling—may be introduced here. The key point applied in these two advanced techniques is related to control of the pattern of ball movement: the former incorporating high-voltage, low-current electrical discharges and the latter using the external magnetic field. In both techniques, the applied conditions cause rapid fracture rates, enhanced mechano-chemical

reactions and novel reaction paths [81][82][83]. However, achieving flake powder using EDAMM and magnetic mechanical milling strongly depends on processing parameters such as discharge type (glow and spark [84]) and operation mode (shearing and impact [82]).

The EDAMM technique works on the principle of interface transformation rather than diffusional transformation, the main underlaying mechanism in conventional BM, as shown in Figure 6a. Indeed, narrow and micro-sized gaps between individual balls, as well as between balls and the chambering wall accompanied by a high-voltage electrical impulse, are basically governed by the type of electrical discharge that is formed. The mechanisms associated with these types of milling with electrical discharge—either glow (cold) or spark (hot)—are highly complex, and more literature on processing parameters under different electrical conditions is required. Moreover, according to the current knowledge, there is a general consensus on the fact that the electrical discharge condition induces large thermal and mechanical stresses within powder particles which, in turn, cause combined effects such as local melting, partial evaporation and Joule heating [81][83][84]. The morphology of the achieved powder has a dominant shape, mostly flake, followed by circular and angular (irregular).
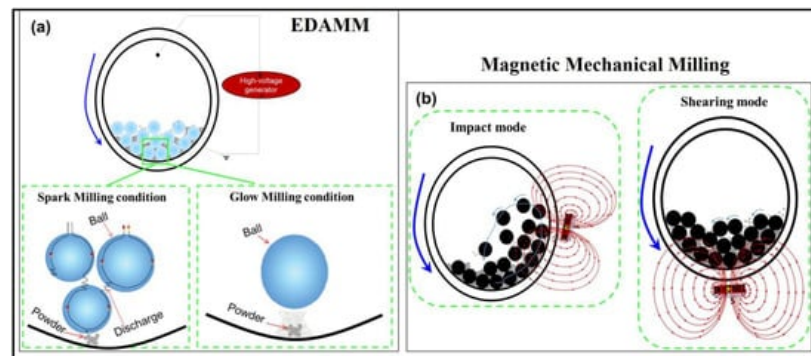

Figure 6. Schematic illustrates of (**a**) electrical discharge-assisted mechanical milling, (**b**) magnetic mechanical milling. With permission of [83].

References

1. Tjong, S.C. Recent progress in the development and properties of novel metal matrix nanocomposites reinforced with carbon nanotubes and graphene nanosheets. Mater. Sci. Eng. R Rep. 2013, 74, 281–350.

2. Choi, H.; Shin, J.; Bae, D. The effect of milling conditions on microstructures and mechanical properties of Al/MWCNT composites. Compos. Part A Appl. Sci. Manuf. 2012, 43, 1061–1072.

3. Cavaliere, P.; Sadeghi, B.; Shabani, A. Carbon nanotube reinforced aluminum matrix composites produced by spark plasma sintering. J. Mater. Sci. 2017, 52, 8618–8629.

4. Salimi, S.; Izadi, H.; Gerlich, A.P. Fabrication of an aluminum–carbon nanotube metal matrix composite by accumulative roll-bonding. J. Mater. Sci. 2010, 46, 409–415.

5. Asgharzadeh, H.; Joo, S.-H.; Kim, H.S. Consolidation of carbon nanotube reinforced aluminum matrix composites by high-pressure torsion. Met. Mater. Trans. A 2014, 45, 4129–4137.

6. Sadeghi, B.; Shamanian, M.; Cavaliere, P.; Ashrafizadeh, F. Effect of processing parameters on the microstructural and mechanical properties of aluminum–carbon nanotube composites produced by spark plasma sintering. Int. J. Mater. Res. 2018, 109, 900–909.

7. Sadeghi, B.; Cavaliere, P.; Perrone, A. Effect of Al2O3, SiO2 and carbon nanotubes on the microstructural and mechan-ical behavior of spark plasma sintered aluminum based nanocomposites. Part. Sci. Technol. 2018, 38, 7–14.

8. Esawi, A.; Morsi, K.; Sayed, A.; Taher, M.; Lanka, S. Effect of carbon nanotube (CNT) content on the mechanical properties of CNT-reinforced aluminium composites. Compos. Sci. Technol. 2010, 70, 2237–2241.

9. Noguchi, T.; Magario, A.; Fukazawa, S.; Shimizu, S.; Beppu, J.; Seki, M. Carbon nanotube/aluminium composites with uniform dispersion. Mater. Trans. 2004, 45, 602–604.

10. Kwon, H.; Estili, M.; Takagi, K.; Miyazaki, T.; Kawasaki, A. Combination of hot extrusion and spark plasma sintering for producing carbon nanotube reinforced aluminum matrix composites. Carbon 2009, 47, 570–577.

11. Yang, X.; Liu, E.; Shi, C.; He, C.; Li, J.; Zhao, N.; Kondoh, K. Fabrication of carbon nanotube reinforced Al composites with well-balanced strength and ductility. J. Alloys Compd. 2013, 563, 216–220.

12. Yang, X.; Zou, T.; Shi, C.; Liu, E.; He, C.; Zhao, N. Effect of carbon nanotube (CNT) content on the properties of in-situ synthesis CNT reinforced Al composites. Mater. Sci. Eng. A 2016, 660, 11–18.

13. Deng, H.; Yi, J.; Xia, C.; Yi, Y. Improving the mechanical properties of carbon nanotube-reinforced pure copper matrix composites by spark plasma sintering and hot rolling. Mater. Lett. 2018, 210, 177–181.

14. Li, Q.Q.; Viereckl, A.; Rottmair, C.A.; Singer, R.F. Improved processing of carbon nanotube/magnesium alloy composites. Compos. Sci. Technol. 2009, 69, 1193–1199.

15. Li, X.; Liu, C.; Ma, M.; Liu, R. Microstructures and mechanical properties of AA6061–SiC composites prepared through spark plasma sintering and hot rolling. Mater. Sci. Eng. A 2016, 650, 139–144.

16. Guo, B.; Ni, S.; Yi, J.; Shen, R.; Tang, Z.; Du, Y.; Song, M. Microstructures and mechanical properties of carbon nanotubes reinforced pure aluminum composites synthesized by spark plasma sintering and hot rolling. Mater. Sci. Eng. A 2017, 698, 282–288.

17. Liu, Z.; Xiao, B.; Wang, W.; Ma, Z. Tensile strength and electrical conductivity of carbon nanotube reinforced alumi-num matrix composites fabricated by powder metallurgy combined with friction stir processing. J. Mater. Sci. Technol. 2014, 30, 649–655.

18. Zabihi, M.; Toroghinejad, M.R.; Shafyei, A. Application of powder metallurgy and hot rolling processes for manu-facturing aluminum/alumina composite strips. Mater. Sci. Eng. A 2013, 560, 567–574.

19. Sadeghi, B.; Cavaliere, P.; Roeen, G.A.; Nosko, M.; Shamanian, M.; Trembošová, V.; Nagy, Š.; Ebrahimzadeh, N. Hot rolling of MWCNTs reinforced Al matrix composites produced via spark plasma sintering. Adv. Compos. Hybrid Mater. 2019, 2, 549–570.

20. Pérez-Bustamante, R.; Gómez-Esparza, C.; Estrada-Guel, I.; Miki-Yoshida, M.; Licea-Jiménez, L.; Pérez-García, S.; Martínez-Sánchez, R. Microstructural and mechanical characterization of Al–MWCNT composites produced by mechanical milling. Mater. Sci. Eng. A 2009, 502, 159–163.

21. Choi, H.; Kwon, G.; Lee, G.; Bae, D. Reinforcement with carbon nanotubes in aluminum matrix composites. Scr. Mater. 2008, 59, 360–363.

22. Bakshi, S.R.; Lahiri, D.; Agarwal, A. Carbon nanotube reinforced metal matrix composites—A review. Int. Mater. Rev. 2010, 55, 41–64.

23. Liu, Z.; Xiao, B.; Wang, W.; Ma, Z. Modelling of carbon nanotube dispersion and strengthening mechanisms in Al matrix composites prepared by high energy ball milling-powder metallurgy method. Compos. Part A Appl. Sci. Manuf. 2017, 94, 189–198.

24. Jiang, L.; Li, Z.; Fan, G.; Cao, L.; Zhang, D. The use of flake powder metallurgy to produce carbon nanotube (CNT)/aluminum composites with a homogenous CNT distribution. Carbon 2012, 50, 1993–1998.

25. Fan, G.; Jiang, Y.; Tan, Z.; Guo, Q.; Xiong, D.-B.; Su, Y.; Lin, R.; Hu, L.; Li, Z.; Zhang, D. Enhanced interfacial bonding and mechanical properties in CNT/Al composites fabricated by flake powder metallurgy. Carbon 2018, 130, 333–339.

26. Jiang, L.; Li, Z.; Fan, G.; Cao, L.; Zhang, D. Strong and ductile carbon nanotube/aluminum bulk nanolaminated composites with two-dimensional alignment of carbon nanotubes. Scr. Mater. 2012, 66, 331–334.

27. Xu, R.; Tan, Z.; Xiong, D.; Fan, G.; Guo, Q.; Zhang, J.; Su, Y.; Li, Z.; Zhang, D. Balanced strength and ductility in CNT/Al composites achieved by flake powder metallurgy via shift-speed ball milling. Compos. Part A Appl. Sci. Manuf. 2017, 96, 57–66.

28. Xu, R.; Fan, G.; Tan, Z.; Ji, G.; Chen, C.; Beausir, B.; Xiong, D.-B.; Guo, Q.; Guo, C.; Li, Z.; et al. Back stress in strain hardening of carbon nanotube/aluminum composites. Mater. Res. Lett. 2017, 6, 113–120.

29. Ye, H.; Liu, X.Y.; Hong, H. Fabrication of metal matrix composites by metal injection molding—A review. J. Mater. Process. Technol. 2008, 200, 12–24.

30. Burmeister, C.F.; Kwade, A. Process engineering with planetary ball mills. Chem. Soc. Rev. 2013, 42, 7660–7667.

31. Witkin, D.; Lavernia, E. Synthesis and mechanical behavior of nanostructured materials via cryomilling. Prog. Mater. Sci. 2006, 51, 1–60.

32. Zhang, Y.; Sabbaghianrad, S.; Yang, H.; Topping, T.D.; Langdon, T.G.; Lavernia, E.J.; Schoenung, J.M.; Nutt, S.R. Two-Step SPD processing of a trimodal al-based nano-composite. Met. Mater. Trans. A 2015, 46, 5877–5886.

33. Ma, K.K.; Wen, H.M.; Hu, T.; Topping, T.D.; Isheim, D.; Seidman, D.N.; Lavernia, E.J.; Schoenung, J.M. Mechanical be-havior and strengthening mechanisms in ultrafine grain precipitation-strengthened aluminum alloy. Acta Mater. 2014, 62, 141–155.

34. Fan, G.; Xu, R.; Tan, Z.; Zhang, D.; Li, Z. Development of Flake Powder Metallurgy in Fabricating Metal Matrix Composites: A Review. Acta Met. Sin. Engl. Lett. 2014, 27, 806–815.

35. Morsi, K.; Esawi, A. Effect of mechanical alloying time and carbon nanotube (CNT) content on the evolution of aluminum (Al)–CNT composite powders. J. Mater. Sci. 2007, 42, 4954–4959.

36. Zan, Y.; Zhou, Y.; Liu, Z.; Ma, G.; Wang, D.; Wang, Q.; Wang, W.; Xiao, B.; Ma, Z. Enhancing strength and ductility synergy through heterogeneous structure design in nanoscale Al2O3 particulate reinforced Al composites. Mater. Des. 2019, 166, 107629.

37. Cao, L.; Li, Z.; Fan, G.; Jiang, L.; Zhang, D.; Moon, W.-J.; Kim, Y.-S. The growth of carbon nanotubes in aluminum powders by the catalytic pyrolysis of polyethylene glycol. Carbon 2012, 50, 1057–1062.

38. Tang, J.; Fan, G.; Li, Z.; Li, X.; Xu, R.; Li, Y.; Zhang, D.; Moon, W.-J.; Kaloshkin, S.D.; Churyukanova, M. Synthesis of car-bon nanotube/aluminium composite powders by polymer pyrolysis chemical vapor deposition. Carbon 2013, 55, 202–208.

39. Jiang, L.; Fan, G.; Li, Z.; Kai, X.; Zhang, D.; Chen, Z.; Humphries, S.; Heness, G.; Yeung, W.Y. An approach to the uniform dispersion of a high volume fraction of carbon nanotubes in aluminum powder. Carbon 2011, 49, 1965–1971.

40. Hu, Y.; Yu, Z.; Fan, G.; Tan, Z.; Zhou, J.; Zhang, H.; Li, Z.; Zhang, D. Simultaneous enhancement of strength and ductility with nano dispersoids in nano and ultrafine grain metals: A brief review. Rev. Adv. Mater. Sci. 2020, 59, 352–360.

41. Xu, R.; Tan, Z.; Fan, G.; Ji, G.; Xiong, D.-B.; Guo, Q.; Su, Y.; Li, Z.; Zhang, D. High-strength CNT/Al-Zn-Mg-Cu composites with improved ductility achieved by flake powder metallurgy via elemental alloying. Compos. Part A Appl. Sci. Manuf. 2018, 111, 1–11.

42. Chen, M.; Fan, G.; Tan, Z.; Xiong, D.; Guo, Q.; Su, Y.; Zhang, J.; Li, Z.; Naito, M.; Zhang, D. Design of an efficient flake powder metallurgy route to fabricate CNT/6061Al composites. Mater. Des. 2018, 142, 288–296.

43. Fu, X.; Tan, Z.; Min, X.; Li, Z.; Yue, Z.; Fan, G.; Xiong, D.-B.; Li, Z. Trimodal grain structure enables high-strength CNT/Al-Cu-Mg composites higher ductility by powder assembly & alloying. Mater. Res. Lett. 2020, 9, 50–57.

44. Shi, Y.; Lu, Y.; Ni, Z.; Zhao, L.; Li, Z.; Xiong, D.-B.; Zou, J.; Guo, Q. Correlation Between Microstructural Architecture and Mechanical Behavior of Single-Walled Carbon Nanotube-Aluminum Composites. Met. Mater. Trans. A 2019, 51, 545–551.

45. Shi, Y.; Zhao, L.; Li, Z.; Li, Z.; Xiong, D.-B.; Su, Y.; Osovski, S.; Guo, Q. Strengthening and deformation mechanisms in nanolaminated single-walled carbon nanotube-aluminum composites. Mater. Sci. Eng. A 2019, 764, 138273.

46. Sadeghi, B.; Cavaliere, P.; Nosko, M.; Trembošová, V.; Nagy, Š. Hot deformation behaviour of bimodal sized Al 2 O 3/Al nanocomposites fabricated by spark plasma sintering. J. Microsc. 2021, 281, 28–45.

47. Sadeghi, B.; Shabani, A.; Cavaliere, P. Hot rolling of spark-plasma-sintered pure aluminium. Powder Met. 2018, 61, 285–292.

48. Bakshi, S.R.; Agarwal, A. An analysis of the factors affecting strengthening in carbon nanotube reinforced aluminum composites. Carbon 2011, 49, 533–544.

49. Sadeghi, B.; Fan, G.; Tan, Z.; Li, Z.; Kondo, A.; Naito, M. Smart mechanical powder processing for producing carbon nanotube reinforced aluminum matrix composites. KONA Powder Part. J. 2020, 2022004.

50. Li, Z.; Guo, Q.; Li, Z.; Fan, G.; Xiong, D.-B.; Su, Y.; Zhang, J.; Zhang, D. Enhanced mechanical properties of graphene (reduced graphene oxide)/aluminum composites with a bioinspired nanolaminated structure. Nano Lett. 2015, 15, 8077–8083.

51. Jiang, Y.; Xu, R.; Tan, Z.; Ji, G.; Fan, G.; Li, Z.; Xiong, D.-B.; Guo, Q.; Li, Z.; Zhang, D. Interface-induced strain hardening of graphene nanosheet/aluminum composites. Carbon 2019, 146, 17–27.

52. Jiang, Y.; Wang, D.; Liang, S.; Cao, F.; Zou, J.; Xiao, P. Effect of local alloying on interfacial bonding in laminated copper matrix composites reinforced by carbon nanotubes. Mater. Sci. Eng. A 2019, 748, 173–179.

53. Yoo, S.J.; Han, S.H.; Kim, W.J. Strength and strain hardening of aluminum matrix composites with randomly dis-persed nanometer-length fragmented carbon nanotubes. Scr. Mater. 2013, 68, 711–714.

54. Esawi, A.; Morsi, K.; Sayed, A.; Gawad, A.A.; Borah, P. Fabrication and properties of dispersed carbon nanotube–aluminum composites. Mater. Sci. Eng. A 2009, 508, 167–173.

55. Zhang, Z.; Li, Z.; Tan, Z.; Zhao, H.; Fan, G.; Xu, Y.; Xiong, D.-B.; Li, Z. Bioinspired hierarchical Al2O3/Al laminated composite fabricated by flake powder metallurgy. Compos. Part A Appl. Sci. Manuf. 2021, 140, 106187.

56. Sadeghi, B.; Shamanian, M.; Ashrafizadeh, F.; Cavaliere, P.; Rizzo, A. Influence of Al2O3 nanoparticles on microstructure and strengthening mechanism of al-based nanocomposites produced via spark plasma sintering. J. Mater. Eng. Perform. 2017, 26, 2928–2936.

57. Cavaliere, P.; Sadeghi, B.; Shamanian, M.; Ashrafizadeh, F. Al-based nanocomposites produced via spark plasma sintering: Effect of processing route and reinforcing phases. In Spark Plasma Sintering of Materials; Springer Science and Business Media: Berlin/Heidelberg, Germany, 2019; pp. 161–190.

58. Sadeghi, B.; Shamanian, M.; Cavaliere, P.; Ashrafizadeh, F.; Sanayei, M.; Szpunar, J.A. Microstructural and mechanical behavior of bimodal reinforced Al-based composites produced by spark plasma sintering and FSP. Int. J. Adv. Manuf. Technol. 2017, 94, 3903–3916.

59. Sadeghi, B.; Cavaliere, P.; Shamanian, M.; Sanayei, M.; Szpunar, J.A.; Nosko, M. Electron backscattered diffraction analysis of friction stir processed nanocomposites produced via spark plasma sintering. J. Microsc. 2018, 271, 145–163.

60. Yuan, C.; Tan, Z.; Fan, G.; Chen, M.; Zheng, Q.; Li, Z. Fabrication and mechanical properties of CNT/Al composites via shift-speed ball milling and hot-rolling. J. Mater. Res. 2019, 34, 2609–2619.

61. Chen, B.; Li, S.; Imai, H.; Jia, L.; Umeda, J.; Takahashi, M.; Kondoh, K. An approach for homogeneous carbon nanotube dispersion in Al matrix composites. Mater. Des. 2015, 72, 1–8.

62. Nam, D.H.; Cha, S.I.; Lim, B.K.; Park, H.M.; Han, D.S.; Hong, S.H. Synergistic strengthening by load transfer mecha-nism and grain refinement of CNT/Al–Cu composites. Carbon 2012, 50, 2417–2423.

63. Cha, S.I.; Kim, K.T.; Arshad, S.N.; Mo, C.B.; Hong, S.H. Extraordinary strengthening effect of carbon nanotubes in metal-matrix nanocomposites processed by molecular-level mixing. Adv. Mater. 2005, 17, 1377–1381.

64. He, N.Z.C.; Shi, C.; Du, X.; Li, J.; Li, H.; Cui, Q. An approach to obtaining homogeneously dispersed carbon nano-tubes in al powders for preparing reinforced al-matrix composites. Adv. Mater. 2007, 19, 1128–1132.

65. Baig, Z.; Mamat, O.; Mustapha, M. Recent progress on the dispersion and the strengthening effect of carbon nanotubes and graphene-reinforced metal nanocomposites: A review. Crit. Rev. Solid State Mater. Sci. 2018, 43, 1–46.

66. Basariya, M.R.; Srivastava, V.C.; Mukhopadhyay, N.K. Microstructural characteristics and mechanical prop-erties of carbon nanotube reinforced aluminum alloy composites produced by ball milling. Mater. Des. 2014, 64, 542–549.

67. Liu, Z.Y.; Xu, S.J.; Xiao, B.L.; Xue, P.; Wang, W.G.; Ma, Z.Y. Effect of ball-milling time on mechanical properties of car-bon nanotubes reinforced aluminum matrix composites. Compos. Part A Appl. Sci. Manuf. 2012, 43, 2161–2168.

68. Suryanarayana, C. Mechanical alloying and milling. Prog. Mater. Sci. 2001, 46, 1–184.

69. Ma, P.C.; Siddiqui, N.A.; Marom, G.; Kim, J.K. Dispersion and functionalization of carbon nanotubes for poly-mer-based nanocomposites: A review. Compos. Part A Appl. Sci. Manuf. 2010, 41, 1345–1367.

70. Xu, R.; Tan, Z.; Fan, G.; Ji, G.; Li, Z.; Guo, Q.; Li, Z.; Zhang, D. Microstructure-based modeling on structure-mechanical property relationships in carbon nanotube/aluminum composites. Int. J. Plast. 2019, 120, 278–295.

71. Azarniya, A.; Azarniya, A.; Sovizi, S.; Hosseini, H.R.M.; Varol, T.; Kawasaki, A.; Ramakrishna, S. Physicomechanical properties of spark plasma sintered carbon nanotube-reinforced metal matrix nanocomposites. Prog. Mater. Sci. 2017, 90, 276–324.

72. Zhang, X.; Zhao, N.; He, C. The superior mechanical and physical properties of nanocarbon reinforced bulk compo-sites achieved by architecture design—A review. Prog. Mater. Sci. 2020, 113, 100672.

73. Cavaliere, P.; Jahantigh, F.; Shabani, A.; Sadeghi, B. Influence of SiO2 nanoparticles on the microstructure and me-chanical properties of Al matrix nanocomposites fabricated by spark plasma sintering. Compos. Part B Eng. 2018, 146, 60–68.

74. Hao, X.-n.; Zhang, H.-p.; Zheng, R.-x.; Zhang, Y.-t.; Ameyama, K.; Ma, C.-l. Effect of mechanical alloying time and rota-tion speed on evolution of CNTs/Al-2024 composite powders. Trans. Nonferrous Met. Soc. China 2014, 24, 2380–2386.

75. Wu, Y.; Kim, G.-Y.; Russell, A.M. Mechanical alloying of carbon nanotube and Al6061 powder for metal matrix composites. Mater. Sci. Eng. A 2012, 532, 558–566.

76. Sadeghi, B.; Shamanian, M.; Ashrafizadeh, F.; Cavaliere, P.; Valerini, D. Nanoindentation characterization of Al-matrix nanocomposites produced via spark plasma sintering. Int. J. Mater. Res. 2018, 109, 50–62.

77. Simoes, S.; Viana, F.; Reis, M.A.L.; Vieira, M.F. Improved dispersion of carbon nanotubes in aluminum nanocompo-sites. Compos. Struct. 2014, 108, 992–1000.

78. Deng, K.-K.; Wang, C.-J.; Nie, K.-B.; Wang, X.-J. Recent research on the deformation behavior of particle reinforced magnesium matrix composite: A review. Acta Met. Sin. Engl. Lett. 2019, 32, 413–425.

79. Jiang, L.; Li, Z.; Fan, G.; Zhang, D. A flake powder metallurgy approach to Al2O3/Al biomimetic nanolaminated composites with enhanced ductility. Scr. Mater. 2011, 65, 412–415.

80. Tan, Z.; Li, Z.; Fan, G.; Li, W.; Liu, Q.; Zhang, W.; Zhang, D. Two-dimensional distribution of carbon nanotubes in copper flake powders. Nanotechnology 2011, 22, 225603.

81. Calka, A.; Wexler, D. Mechanical milling assisted by electrical discharge—Recent developments. J. Metastable Nanocryst. Mater. 2004, 20–21, 111–117.

82. Calka, A.; Radlinski, A.P. Universal high performance ball-milling device and its application for mechanical alloy-ing. Mater. Sci. Eng. A 1991, 134, 1350–1353.

83. Calka, A.; Wexler, D. Mechanical milling assisted by electrical discharge. Nat. Cell Biol. 2002, 419, 147–151.

84. Cavaliere, P.; Sadeghi, B.; Shabani, A. Spark Plasma Sintering: Process Fundamentals. In Spark Plasma Sintering of Materials; Springer: Cham, Switzerland, 2019; pp. 3–20.